

Dominance of direct reaction channels at deep sub-barrier energies for weakly bound nuclei on heavy targets: The case ${}^8\text{B} + {}^{208}\text{Pb}$

A. Pakou^{1,*}, L. Acosta,² P. D. O'Malley,³ S. Aguilar,³ E. F. Aguilera,⁴ M. Baines,³ D. Bardayan,³ F. D. Becchetti,⁵ Ch. Boomershine,³ M. Brodeur,³ F. Cappuzzello,^{6,7} S. Carmichael,³ L. Caves,³ E. Chávez,² C. Flores-Vázquez,² A. Gula,³ J. J. Kolata,³ B. Liu,³ D. J. Marín-Lámbarrí,² F. F. Morales,² K. Rusek,⁸ A. M. Sánchez-Benítez,⁹ O. Sgouros,⁶ V. R. Sharma,⁴ V. Soukeras,⁶ and G. Souliotis¹⁰

¹*Department of Physics and HINP, The University of Ioannina, 45110 Ioannina, Greece*

²*Instituto de Física, Universidad Nacional Autónoma de México, Apartado 20-364, Mexico City 01000, Mexico*

³*Department of Physics, University of Notre Dame, Notre Dame, Indiana 46556, USA*

⁴*Departamento de Aceleradores, Instituto Nacional de Investigaciones Nucleares, Apartado Postal 18-1027, Código Postal 11801, Mexico, Distrito Federal, Mexico*

⁵*Department of Physics, University of Michigan, Ann Arbor, Michigan 48109, USA*

⁶*INFN Laboratori Nazionali del Sud, via S. Sofia 62, 95125, Catania, Italy*

⁷*Dipartimento di Fisica e Astronomia, Università di Catania, via S. Sofia 64, 95125, Catania, Italy*

⁸*Heavy Ion Laboratory, University of Warsaw, ulica Pasteura 5a, 02-093, Warsaw, Poland*

⁹*Department of Integrated Sciences, Centro de Estudios Avanzados en Física, Matemáticas y Computación (CEAFMC), University of Huelva, 21071 Huelva, Spain*

¹⁰*Department of Chemistry, National and Kapodistrian University of Athens and HINP, 15771 Athens, Greece*



(Received 22 May 2020; accepted 11 August 2020; published 23 September 2020)

We report the first evidence of breakup dominance at deep sub-barrier energies for the proton halo nucleus ${}^8\text{B}$ on a heavy target. Angular distribution measurements of the ${}^8\text{B}$ breakup fragment, ${}^7\text{Be}$, on lead were performed at the *TwinSol* facility of the University of Notre Dame at a beam energy of 30 MeV, 58% of the Coulomb barrier and corresponding to a distance of closest approach of 20.5 fm. The ${}^7\text{Be}$ yield was observed in two double sided silicon strip detector telescopes symmetrical to the radioactive beam and normalized using the ${}^8\text{B}$ Rutherford scattering. The results are in excellent agreement with continuum discretized coupled channel calculations with a total breakup cross section (326 ± 84) mb. This is found to exhaust all of the total reaction cross section for the system ${}^8\text{B} + {}^{208}\text{Pb}$, possibly prohibiting a fusion enhancement. This finding is expected to give more insight to the puzzle of fusion suppression at deep sub-barrier energies with possible major consequences on nuclear astrophysics.

DOI: [10.1103/PhysRevC.102.031601](https://doi.org/10.1103/PhysRevC.102.031601)

The application of quantum mechanics finds fertile ground on several research disciplines as chemistry, solid-state and nuclear physics. For example, tunneling is a well known quantum-mechanical process where a subatomic particle passes through a potential barrier. This phenomenon plays an essential role in several aspects of the above disciplines with applications such as the tunnel diode, quantum computing, scanning microscopes, on radioactivity, and nuclear fusion. The application of tunneling on nuclear fusion is not a straightforward task. Various properties of the nucleus with a particular structure, intrinsic degrees of freedom and competing reactions, or/and the saturation properties of nuclear matter and the Pauli exclusion principle, affect strongly this phenomenon. Several review articles unfold until today the existing situation [1–6].

The concept of the strong short-range nuclear potential and various phenomena in nuclear astrophysics had led to

the idea of nuclear reactions at lower energies proceeding mainly through a compound nucleus formation or at least that this constitutes a major part of the reaction cross section. However, other mechanisms even if they are minimal may be very important. At much higher energies than the Coulomb barrier, geometrical models can independently describe compound and direct mechanisms. This is no longer valid for near barrier and below barrier energies. Coupled channel approaches have been developed to interpret large enhancements on below barrier fusion of heavy nuclei due to the structure of the involved colliding nuclei and competing direct reaction processes [4,7–11]. At deep sub-barrier energies and below the region that is well described by standard coupled-channels theories, a fusion hindrance was established for heavy systems [12–22]. On the other hand, the case of light and especially weakly bound nuclei, and further on halo nuclei, is even more complicated due to the onset of breakup and transfer effects even at very low energies. Existing experimental data are scarce and mostly unclear. The effect of the neutron and proton halo on fusion could include a large enhancement due

*apakou@uoi.gr

to the fact that nuclear matter extends much further than the usual interaction distance, but alternatively the weak binding energy of the nuclei could inhibit the process. Due to the weak binding of ${}^6\text{He}$, a large α particle yield attributed to direct processes is reported in 2000 in Ref. [23], which below barrier exhausts almost all the reaction cross section. The dominance of transfer at the expense of fusion is reported for ${}^6\text{He} + {}^{238}\text{U}$ in 2004 [24] and later on in 2009 for ${}^8\text{He} + {}^{197}\text{Au}$ [25]. The onset of direct mechanisms for neutron halo nuclei at below barrier energies is now apparent but not yet well understood. The question arising here concerns the proton halo nuclei. Are they going to have the same behavior? Among them, ${}^8\text{B}$ is a proton drip line β -decaying nucleus, attracting a strong interest due to its role in the production of high-energy neutrinos in the sun [26–29] and its unusual structure with a possible proton halo [30,31]. For this nucleus, at around the same time, Continuum Discretized Coupled Channel (CDCC) calculations are reported [31] indicating a large breakup cross section below barrier which exhausts the total reaction cross section. This was a very interesting result since transfer processes were found to dominate the total reaction cross section below barrier for ${}^6,8\text{He}$. However their Q value is positive, while the breakup for ${}^8\text{B}$ has a negative Q value albeit very close to zero. Further on, a sound result which motivates the present Rapid Communication, is reported in 2015 in Ref. [32]. In that investigation, ratios of direct to total reaction cross sections are deduced as upper limits from experimental data of weakly bound nuclei, appropriately scaled, and an energy mapping of these ratios is performed at near and sub-barrier energies. It is found that although at near-barrier energies this ratio is similar for weakly bound nuclei on all targets and close to $\approx 20\%$ for energies below the barrier the ratio is target dependent and saturates to $\approx 70\%$ for light targets ($A = 28$), to $\approx 80\%$ for medium mass targets ($A = 90$), and to almost $\approx 100\%$ for heavy targets ($A = 208$), leaving little room in the last case for fusion. If this prediction can be further validated experimentally it will have important consequences for the fusion mechanism itself and for various related astrophysical problems. No fusion measurements for the proton halo nucleus ${}^8\text{B}$ on heavy targets exist, but rather on the low mass target ${}^{28}\text{Si}$ [33] at above-barrier energies exhibiting a rather standard behavior and on a medium mass target ${}^{58}\text{Ni}$ [34] at below-barrier energies, exhibiting a large fusion enhancement. For the proton-rich nucleus ${}^7\text{Be}$, measurements on medium mass targets show an enhancement below and above the barrier [35], while for ${}^7\text{Be}$ on a heavy target ${}^{238}\text{U}$, no strong enhancement is observed for complete fusion below the barrier and a suppression is reported for above-barrier energies [36]. A total reaction cross-section measurement is reported for ${}^8\text{B} + {}^{208}\text{Pb}$ in Ref. [37], larger than usual cross sections for other proton-rich nuclei but compatible with CDCC calculations. Further on at near-barrier energies, the only existing breakup measurement for ${}^8\text{B}$ at 25.7 MeV, corresponding to 1.08 times the Coulomb barrier ($E_{\text{C.b.-lab}} = 23.7$ MeV according to Broglia and Winther [38]) and related with a distance of the closest approach of 8.9 fm, is performed on a ${}^{58}\text{Ni}$ target with a large cross section observed, exhausting at least 50% of the total reaction cross section [39,40]. This breakup result is also consistent with CDCC calculations [41].

Motivated by all the above, taking into account the experimental data in the above-mentioned systematic investigation [32] and the theoretical prediction in a CDCC framework [31] we have undertaken a direct reaction channel measurement, the breakup for ${}^8\text{B} + {}^{208}\text{Pb}$. The nucleus ${}^8\text{B}$ gives us a unique possibility to obtain the direct part of the total reaction cross section at energies below the barrier and indeed at deep sub-barrier energies where the distance of closest approach is 20.5 fm. This distance is at least two times the sum of radii of the two colliding nuclei ${}^8\text{B}$ and ${}^{208}\text{Pb}$ ($R_1 + R_2 = 9.5$ fm with $R = 1.2 * A^{1/3}$). Proton transfer is evaluated to be less than 1% and the expected breakup at the low energy of 30 MeV ($E_{\text{C.b.-lab}} = 51.7$ MeV) is $\sigma_{\text{break}}^{\text{CDCC}} = 300$ mb, a substantial value that can be measured even under the difficult technical conditions of the production of this rare radioactive beam. The measurement can be inclusive, observing the ${}^7\text{Be}$ yield, which as mentioned above is only due to the breakup process. The ${}^8\text{B}$ beam has to be clear of other beam particles and especially ${}^7\text{Be}$, and at the appropriate low energy, and this is possible at the *TwinSol* facility [42].

Our experiment was carried out at the Nuclear Science Laboratory of the University of Notre Dame (UND). The ${}^8\text{B}$ beam was produced at the *TwinSol* facility [42] by using the two-proton transfer reaction ${}^6\text{Li} + {}^3\text{He}$. A primary bunched beam of ${}^6\text{Li}$ was accelerated at 37 MeV at the UND FN tandem and impinged on a gas target of ${}^3\text{He}$ at a pressure of 1 atm. The reaction products included in the secondary beam were ${}^7\text{Li}$ at 13.1 MeV, ${}^7\text{Be}$ at 22.4 MeV and ${}^8\text{B}$ at the energy of 30.5 MeV. The secondary beams and part of the scattered primary ${}^6\text{Li}$ beam were transported via solenoids and focused on a natural lead target, 2.2 mg/cm² thick. The ${}^8\text{B}$ beam flux was ≈ 5000 pps, lower by far from other experiments in the *TwinSol* facility due to some technical problems in producing the ${}^6\text{Li}$ primary beam at an adequate intensity. Elastically scattered and reaction products were detected by two silicon telescopes, set at almost symmetrical positions to the beam from the Sistema Móvil de Alta Segmentación (SIMAS) array of the Laboratorio Nacional de Espectrometría de Masas con Aceleradores, the National Laboratory of the Physics Institute at the Autonomous National University of Mexico. Each telescope included a double-sided silicon strip detector (DSSSD) with nominal thickness of ≈ 20 μm (the effective thickness of each strip was estimated during the run and calibrations to be 24 ± 4 μm), backed by a silicon pad 150- μm thick. One telescope was set beam left covering an angular range between $\approx 25.8^\circ$ and 69.2° , being 59.9 mm far away from the lead target, while the second telescope was set beam right covering an angular range between $\approx 28.5^\circ$ and 66.5° being 69.95 mm away from the target.

A crucial aspect of that experiment was a good separation between the secondary beams ${}^8\text{B}$ and ${}^7\text{Be}$. This was achieved in an excellent way by imposing a time of flight (TOF) requirement. The TOF of the particles was obtained from the time difference between the occurrence of an energy signal in the first stage of each telescope (OR signal of all strips) and the rf timing pulse from the beam buncher. A TOF spectrum versus the energy loss in $\Delta E + E$ of the left beam telescope is shown in Fig. 1(a). As can be seen, the time separation is excellent between the two species. This is also demonstrated

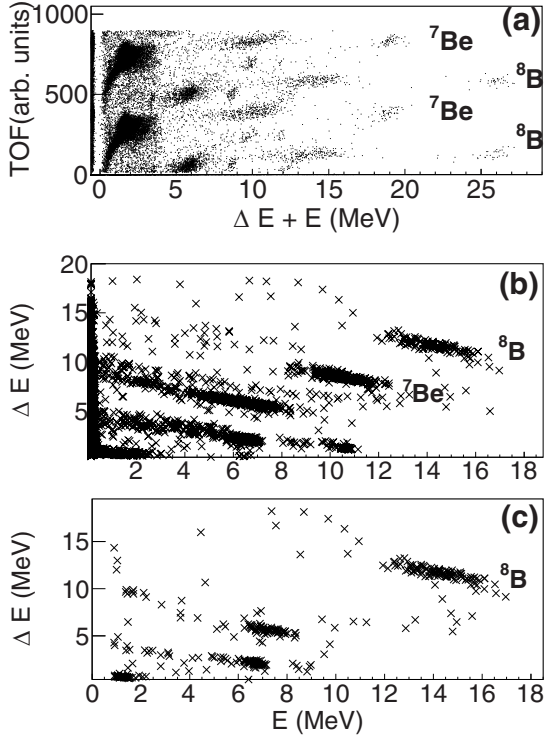


FIG. 1. (a) TOF: $\Delta E + E$ spectrum illustrating the time separation between elastic boron and beryllium events; (b) $\Delta E - E$ spectrum of the left beam telescope for strip 4 (34.65°); (c) the same spectrum but with a TOF restriction to the ^8B beam.

in Figs. 1(b) and 1(c). In Fig. 1(b) a $\Delta E - E$ spectrum is shown without a time window and in Fig. 1(c) the same spectrum but with a time window on ^8B . Apparently all events of the secondary ^7Be beam have been eliminated. Due to the strip nonuniformity of the DSSSD detectors and despite the low intensity of the beam, the analysis was performed pixel by pixel to define in the most accurate way the contour of breakup events. First indication of the contour position was given from the elastic ^7Be events, overlapped in our spectra, solely for guiding the eye. Detailed simulations were also at our disposal for this choice [43,44]. Sample bidimensional spectra are shown in Fig. 2 for two different angles at 34.7° and 51.8° . The obtained breakup events were transformed to cross sections using for normalization purposes the ^8B elastic scattering, according to the following formula

$$\sigma_{\text{break}}(\theta) = \frac{N_{\text{break}}(\theta) * \sigma_{\text{Ruth}}(\theta)}{N_{\text{Ruth}}(\theta)} \quad (1)$$

where $\sigma_{\text{break}}(\theta)$, $\sigma_{\text{Ruth}}(\theta)$ are the differential cross sections of the breakup events the boron elastically scattered (Rutherford scattering), respectively, and $N_{\text{break}}(\theta)$, $N_{\text{Ruth}}(\theta)$ are the breakup ^7Be events and boron elastic events, respectively, at each angle θ . The differential cross sections determined in this way, are independent of the beam flux, target thickness, and solid angle. The assumption for Rutherford scattering for ^8B is valid since according to our calculations coupling to continuum can change at most the elastic-scattering results

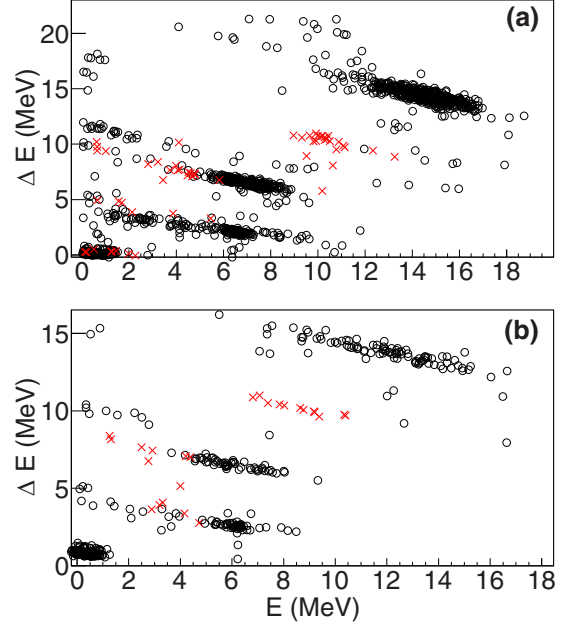


FIG. 2. $\Delta E - E$ spectra with a time window on ^8B ; (a) two middle pixels of strip 4 (34.7°); (b) two middle pixels of strip 10 (51.8°). The \times 's (in red) are elastic-scattering events of ^7Be , overlapped to the spectra in order only to guide the eye for the energy position of the ^7Be breakup events.

by 3%, a slight deviation which cannot be observed in an experiment. Apparently, the behavior of a proton halo nucleus is very different from the one with a neutron halo, e.g., for elastic scattering of ^{11}Li on lead a strong coupling to the continuum caused a big deviation from Rutherford [45]. We have thus repeated our cross-section calculations taking into account the elastic scattering of ^7Be , and the obtained results were similar.

The differential cross sections obtained in this respect were transformed from the laboratory to the center-of-mass (c.m.) system taking into account an inelastic process through the continuum of ^8B , adopting the CDCC binning ($^8\text{B} + ^{208}\text{Pb} \rightarrow ^8\text{B}^* + ^{208}\text{Pb} \rightarrow ^7\text{Be} + p + ^{208}\text{Pb}$). A mean energy was defined for each angular bin, and the appropriate Jacobian extracted. Our experimental angular distribution is compared with the CDCC calculation in Fig. 3, and a very good agreement is observed. A similar calculation is reported in Ref. [31]. Few points, pertinent in this Rapid Communication for the 30-MeV case are given here. The $^7\text{Be} + p$ continuum was discretized into bins in momentum (k) space of width $\Delta k = 0.1 \text{ fm}^{-1}$ and truncated at a value of $k_{\text{max}} = 0.4 \text{ fm}^{-1}$, corresponding to a ^8B “excitation energy” of 3.96 MeV. All values of the $p + ^7\text{Be}$ relative angular momentum L up to $L = 6\hbar$ and couplings up to multipolarity $\lambda = 6$ were included. A matching radius of 400 fm, an integration step size of 0.055 fm and a total of 850 partial waves were required to give a converged result for the breakup cross section. The calculations did not include any resonant states. However, test calculations confirmed that this omission has a negligible effect on the results.

As might be expected at this deep sub-barrier energy, the calculated breakup cross section is essentially independent

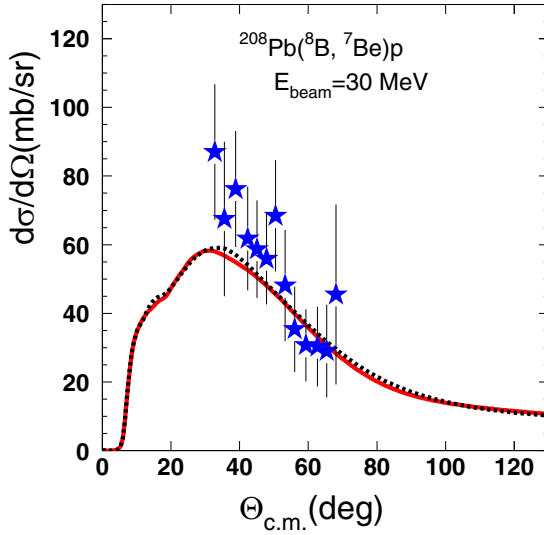


FIG. 3. Angular distribution of the observed ${}^8\text{B} \rightarrow {}^7\text{Be} + p$ breakup yield on a lead target at an ${}^8\text{B}$ incident energy of ≈ 30 MeV (middle of the target). The solid and dashed curves denote the summed breakup angular distributions from the full (Coulomb plus nuclear potentials) and Coulomb potentials only CDCC calculations, respectively, as described in the text.

of the choice of ${}^7\text{Be} + {}^{208}\text{Pb}$ and $p + {}^{208}\text{Pb}$ optical potential parameters used as input to the Watanabe-type folding procedure employed to obtain the ${}^8\text{B} + {}^{208}\text{Pb}$ diagonal and coupling potentials. Indeed, a Coulomb-only calculation gives almost identical results to those including the nuclear breakup, see the dashed curve in Fig. 3. The calculations presented in Fig. 3 as the solid curve used the same $p + {}^{208}\text{Pb}$ potential parameters as Ref. [37] and the global ${}^6\text{Li}$ parameters of Cook [47] for the ${}^7\text{Be} + {}^{208}\text{Pb}$ potential. These give a total integrated breakup cross section of 300 mb and a reaction cross section of 316 mb. The calculation with Coulomb potentials only gives a total integrated breakup cross section of 305 mb, necessarily equal to the reaction cross section in this case since there are no imaginary nuclear potentials and thus no absorption cross section. We should underline here that the energy of calculation and measurement corresponds to a distance of closest approach of 20.5 fm that is over than twice the sum of radii of the colliding nuclei, indicating mainly a pure Coulomb interaction. The integration of the data, extrapolating to more forward and backward angles taking into account the shape of the CDCC angular distribution, gives an experimental breakup cross section, equal to $\sigma_{\text{break}}^{\text{exp}} = (326 \pm 84)$ mb in excellent agreement with the calculation. We should point out here that our value may include incomplete fusion (p capture) which cannot be determined in the present inclusive experiment.

Indeed, we have obtained for the first time a breakup cross section for the ${}^8\text{B} + {}^{208}\text{Pb}$ system at deep sub-barrier energies related with a distance of closest approach equal to 20.5 fm, twice the sum of the colliding nuclei radii. We should underline here that the only other existing breakup measurement of ${}^8\text{B}$ was performed at a ${}^{58}\text{Ni}$ target and a near-barrier energy corresponding to a distance of closest approach

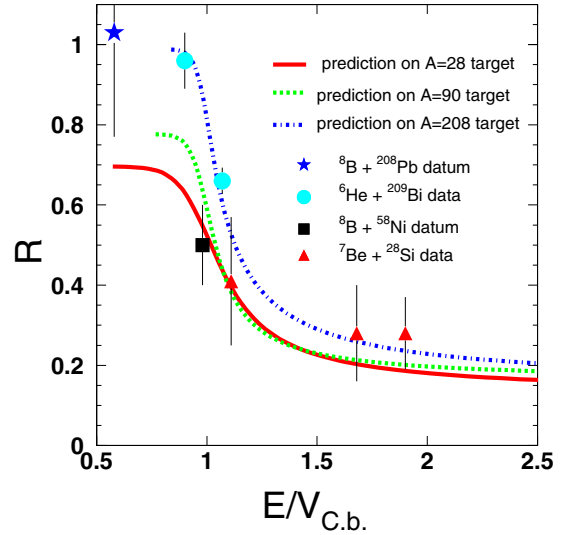


FIG. 4. Ratio's R direct to total reaction cross section. Lines correspond to predictions obtained earlier [32] from experimental data of weakly bound neutron-rich nuclei for various targets, appropriately reduced (red-solid: $A = 28$; green-dotted: $A = 90$; blue-dotted-dashed: $A = 208$). The present experimental datum for ${}^8\text{B} + {}^{208}\text{Pb}$ is designated with the blue star. A previous datum ${}^8\text{B} + {}^{58}\text{Ni}$ is designated with a black box [39,40], while previous data for ${}^7\text{Be} + {}^{28}\text{Si}$ [46] are designated with the red filled arrows, and ${}^6\text{He} + {}^{209}\text{Bi}$ data with cyan filled circles [23].

of 8.9 fm, close to the sum of radii for the colliding nuclei ($R_1 + R_2 = 7.03$ fm). In our case breakup is the only direct process at deep sub-barrier energies and our results, despite the large uncertainties accommodate in an excellent way the CDCC calculation, and the breakup cross section saturates all of the calculated total reaction cross section ($\sigma_{\text{rea}} = 316$ mb). This indicates a very small fusion cross section at these deep-sub-barrier energies. According to Ref. [48] there is a strong correlation between the touching point energy between the two colliding nuclei and the threshold energy where fusion hindrance occurs. Our energy at $E_{\text{c.m.}} = 28.9$ MeV, is well below the touching point energy, calculated to be 42.3 MeV taking into account the proximity potential [49]. This implies that the projectile touching the target is still in the classically forbidden region which involves the penetration of a residual Coulomb barrier [48] resulting in a hindered fusion cross section. We note also that from fusion hindrance systematics [50], the threshold energy where hindrance starts to appear is $E_s = 35.2$ MeV. Therefore, our system at our particular energy, corresponding to a distance of closest approach of 20.5 fm, twice the sum of the colliding nuclei radii, would have been a good candidate to present a fusion hindrance. This cannot be confirmed from present experimental data especially since we lack an experimental total reaction cross-section value from which to deduce an experimental fusion cross section.

However, one thing is confirmed and sound. At deep sub-barrier energies for halo nuclei on heavy targets, the direct reaction channel is dominant. For ${}^8\text{B}$ this channel is breakup despite its negative Q value. Moreover, both results for proton halo and neutron halo data corroborate our previous empirical prediction [32] where ratios of direct to total for weakly bound

nuclei on heavy targets are close to unity. Our present datum for breakup divided by the total reaction cross section of the CDCC calculation is close to unity. This is shown in Fig. 4 in comparison with the predictions. Other experimental data for ${}^6\text{He} + {}^{209}\text{Bi}$ [23] are also shown and compared in an excellent way with the prediction. In good agreement are also data for ${}^8\text{B} + {}^{58}\text{Ni}$ [39,40] and ${}^7\text{Be} + {}^{28}\text{Si}$ in medium and light targets. With the upgrading of *TwinSol* to *TriSol* in the near future, we intend to extend our measurements to medium-heavy targets and validate further this interesting empirical prediction, which needs more investigation from the experimental and theoretical point of view. A more challenging measurement

though, will be a fusion measurement for ${}^8\text{B} + {}^{208}\text{Pb}$ at the present energy of 30 MeV, and we intend to make an attempt in that direction. This might be accessible if fusion is not suppressed and follows the CDCC calculation.

This Rapid Communication was partially supported by the U.S. National Science Foundation: Grants No. PHY-1713857 and No. PHY14-01343 and by CONACyT 299073 and Grants No. CB-01-254619 and No. DGAPA-PAPIIT IN107820 and AG101120 of Mexico. The authors want to warmly thank to A. Huerta-Hernández and M. Pérez-Vielma for their technical support in the construction of the SIMAS array.

-
- [1] J. F. Liang and C. Signorini, *Int. J. Mod. Phys. E* **14**, 1121 (2005).
 - [2] L. F. Canto, P. R. S. Gomes, R. Donangelo, and M. S. Hussein, *Phys. Rep.* **424**, 1 (2006).
 - [3] N. Keeley, R. Raabe, N. Alamanos, and J. L. Sida, *Prog. Part. Nucl. Phys.* **59**, 579 (2007).
 - [4] K. Hagino and N. Takigawa, *Prog. Theor. Phys.* **128**, 1001 (2012).
 - [5] B. B. Back, H. Esbensen, C. L. Jiang, and K. E. Rehm, *Rev. Mod. Phys.* **86**, 317 (2014).
 - [6] J. J. Kolata, V. Guimaraes, and E. F. Aguilera, *Eur. Phys. J. A* **52**, 123 (2016).
 - [7] R. G. Stokstad *et al.*, *Phys. Rev. Lett.* **41**, 465 (1978).
 - [8] C. H. Dasso, S. Landowne, and A. Winther, *Nucl. Phys.* **A405**, 381 (1983).
 - [9] M. J. Rhoades-Brown and P. Braun-Munzinger, *Phys. Lett.* **136B**, 19 (1983).
 - [10] M. Beckerman, *Rep. Prog. Phys.* **51**, 1047 (1988).
 - [11] M. Dasgupta *et al.*, *Annu. Rev. Nucl. Part. Sci.* **48**, 401 (1998).
 - [12] C. L. Jiang *et al.*, *Phys. Rev. Lett.* **89**, 052701 (2002).
 - [13] C. L. Jiang *et al.*, *Phys. Rev. Lett.* **93**, 012701 (2004).
 - [14] C. L. Jiang *et al.*, *Phys. Rev. C* **71**, 044613 (2005).
 - [15] C. L. Jiang *et al.*, *Phys. Lett. B* **640**, 18 (2006).
 - [16] C. L. Jiang *et al.*, *Phys. Rev. C* **78**, 017601 (2008).
 - [17] C. L. Jiang *et al.*, *Phys. Rev. C* **81**, 024611 (2010).
 - [18] C. L. Jiang, A. M. Stefanini, H. Esbensen, K. E. Rehm, L. Corradi, E. Fioretto, P. Mason, G. Montagnoli, F. Scarlassara, R. Silvestri, P. P. Singh, S. Szilner, X. D. Tang, and C. A. Ur, *Phys. Rev. C* **82**, 041601(R) (2010).
 - [19] G. Montagnoli *et al.*, *Phys. Rev. C* **82**, 064609 (2010).
 - [20] G. Montagnoli *et al.*, *Phys. Rev. C* **85**, 024607 (2012).
 - [21] G. Montagnoli *et al.*, *Phys. Rev. C* **87**, 014611 (2013).
 - [22] D. Montanari *et al.*, *Phys. Rev. C* **84**, 054613 (2011).
 - [23] E. F. Aguilera *et al.*, *Phys. Rev. Lett.* **84**, 5058 (2000).
 - [24] R. Raabe *et al.*, *Nature (London)* **431**, 823 (2004).
 - [25] A. Lemasson *et al.*, *Phys. Rev. Lett.* **103**, 232701 (2009).
 - [26] C. A. Bertulani, *Phys. Rev. C* **49**, 2688 (1994).
 - [27] J. von Schwarzenberg, J. J. Kolata, D. Peterson, P. Santi, M. Belbot, and J. D. Hinfefeld, *Phys. Rev. C* **53**, 2598(R) (1996).
 - [28] H. Esbensen, G. F. Bertsch, and K. A. Snover, *Phys. Rev. Lett.* **94**, 042502 (2005).
 - [29] F. Schumann *et al.*, *Phys. Rev. C* **73**, 015806 (2006).
 - [30] E. F. Aguilera, E. Martinez-Quiroz, D. Lizcano, A. Gomez-Camacho, J. J. Kolata, L. O. Lamm, V. Guimaraes, R. Lichtenthaler, O. Camargo, F. D. Becchetti, H. Jiang, P. A. DeYoung, P. J. Mears, and T. L. Belyaeva, *Phys. Rev. C* **79**, 021601(R) (2009).
 - [31] N. Keeley, N. Alamanos, K. W. Kemper, and K. Rusek, *Prog. Part. Nucl. Phys.* **63**, 396 (2009).
 - [32] A. Pakou *et al.*, *Eur. Phys. J. A* **51**, 55 (2015).
 - [33] A. Pakou *et al.*, *Phys. Rev. C* **87**, 014619 (2013).
 - [34] E. F. Aguilera *et al.*, *Phys. Rev. Lett.* **107**, 092701 (2011).
 - [35] E. Martinez-Quiroz *et al.*, *Phys. Rev. C* **90**, 014616 (2014).
 - [36] R. Raabe, C. Angulo, J. L. Charvet, C. Jouanne, L. Nalpas, P. Figuera, D. Pierrousakou, M. Romoli, and J. L. Sida, *Phys. Rev. C* **74**, 044606 (2006).
 - [37] M. Mazzocco *et al.*, *Phys. Rev. C* **100**, 024602 (2019).
 - [38] R. A. Broglia and A. Winther, *Heavy Ion Reactions, Elastic and Inelastic Reactions* (Benjamin/Cummings, San Francisco, 1981), Vol. 1.
 - [39] V. Guimarães, J. J. Kolata, D. Peterson, P. Santi, R. H. White-Stevens, S. M. Vincent, F. D. Becchetti, M. Y. Lee, T. W. O'Donnell, D. A. Roberts, and J. A. Zimmerman, *Phys. Rev. Lett.* **84**, 1862 (2000).
 - [40] J. J. Kolata *et al.*, *Phys. Rev. C* **63**, 024616 (2001).
 - [41] J. A. Tostevin, F. M. Nunes, and I. J. Thompson, *Phys. Rev. C* **63**, 024617 (2001).
 - [42] M. Y. Lee *et al.*, *Nucl. Instrum. Methods Phys. Res., Sect. A* **422**, 536 (1999).
 - [43] A. Matta, P. Morfouace, N. De Sereville, F. Flavigny, M. Labiche, and R. Shearman, *J. Phys. G: Nucl. Part. Phys.* **43**, 045113 (2016).
 - [44] O. Sgouros, V. Soukeras, and A. Pakou, *Eur. Phys. J. A* **53**, 165 (2017).
 - [45] M. Cubero *et al.*, *Phys. Rev. Lett.* **109**, 262701 (2012).
 - [46] O. Sgouros *et al.*, *Phys. Rev. C* **94**, 044623 (2016).
 - [47] J. Cook, *Nucl. Phys.* **A388**, 153 (1982).
 - [48] T. Ichikawa, K. Hagino, and A. Iwamoto, *Phys. Rev. C* **75**, 064612 (2007).
 - [49] W. D. Myers and W. J. Swiatecki, *Phys. Rev. C* **62**, 044610 (2000).
 - [50] C. I. Jiang, B. B. Back, H. Esbensen, R. V. F. Janssens, and K. E. Rehm, *Phys. Rev. C* **73**, 014613 (2006).